

SEMI-DISCRETE SIMULATION OF INTERFACE BEHAVIOR DURING SINGLE FIBER PULL-OUT WITH APPLICATION TO DYNAMICALLY LOADED FIBER-REINFORCED CEMENTITIOUS COMPOSITES

BONHWI CHOO^{*}, KYUWON KIM^{*}, MOON KYUM KIM^{*} AND YUN MOOK LIM[†]

^{*} Department of Civil and Environmental Engineering, College of Engineering, Yonsei University
50, Yonsei-ro, Seodaemun-gu, Seoul, Republic of Korea
e-mail: tsou3328@yonsei.ac.kr; kyu_won@yonsei.ac.kr; applymkk@yonsei.ac.kr

[†] Department of Civil and Environmental Engineering, College of Engineering, Yonsei University
50, Yonsei-ro, Seodaemun-gu, Seoul, Republic of Korea
e-mail: yunmook@yonsei.ac.kr

Key words: Rigid-Body-Spring-Network(RBSN), rate dependency, fiber pullout, semi-discrete

Abstract: In this study, an irregular lattice model is developed to simulate the failure behavior of fiber-reinforced cementitious composites (FRCCs) subjected to extreme loadings with various strain rates. The numerical method is based on the Rigid-Body-Spring-Network(RBSN), which is an irregular lattice model. The matrix of material domain is discretized by the Delaunay/Voronoi dual tessellation, and the lattice nodes are connected by spring sets. Generally, cementitious materials are rate dependent, meaning that their mechanical properties change according to the rates of loading [1-3]. In dynamic failure analysis, considering the rate dependency, the response of a material is obtained in every time step by using, for example, explicit time integration schemes. During the numerical analysis, in order to achieve this material characteristic, a rheological unit, which contains springs and dashpots, is adopted into the rigid-body-spring elements of the lattice model [4, 5]. The rheological unit represents sources of rate dependency, including inertia of mass and Stepan's effects. In the previous researches, the strain rate dependency was shown for plain concrete and expanded to the case of reinforced concrete. In this research, the method to handle the interface property, which is rate sensitive, are demonstrated for the case of fiber pull-out from a cementitious matrix. A semi-discrete method is chosen since fiber addition does not add degrees of freedom(DOF) into the lattice model [6, 7]. This method is computationally efficient since no additional DOF are introduced when adding fibers to the matrix. In this paper, we are focusing on the interface for a single fiber with several RBSN cells to check the developed algorithm. To identify the correlation between the interfacial properties and the overall failure behavior of FRCCs under different loading rates, related parameter studies are fully conducted.

1 INTRODUCTION

Recently, the number of researches on increasing the durability and ductility of civil infrastructures against extreme loads such as earthquakes and explosions is increasing. Because the tensile strength of concrete is generally one-tenth of its compressive strength, cracks are regularly generated against tensile

loads, and post-cracking response is quasi-brittle. Therefore, reinforcing steels are embedded in concrete to increase its tensile strength. However, brittle failures such as spalling and fragment are still often visible on reinforced concrete (RC) structures concrete when an impact or a blast loading is applied [8]. In order to increase the safety of RC structures,

concrete's ductility has to be increased. Accordingly, FRCCs, in which fibers provide tensile ductility, have been developed. With the development of different kinds of FRCCs, analysis methods to describe the behavior of FRCCs have been developed; however, most of the method are for analyzing static loading behavior. In this study, an established analysis method is extended to describe rate dependency of the fiber, matrix and the interface between them.

2 METHODOLOGY

2.1 Rigid-Body-Spring-Network(RBSN)

RBSN is a type of irregular lattice model that is based on a set of rigid particles interconnected by springs. It was first proposed by Kawai, and its mesh is generated in the following order: (1) random point generation in the domain; (2) Delaunay tessellation of the point set; and (3) Voronoi tessellation (Figure 1). Random mesh is a sufficient way to express the heterogeneity of concrete. The Voronoi cells are considered as a rigid body, and two adjacent random nodes, i and j , are connected to a centroid point, c , which is on a Voronoi facet, by a zero-size spring set that has 6 degrees of freedom (Figure 2). The stiffness of the spring set to the translational motion at the three individual local axis can be expressed as follows:

$$k_n = \frac{E(1-\nu)}{(1+\nu)(1-\nu)} \frac{A_{ij}}{h_{ij}} \quad (1)$$

$$k_s = k_t = \frac{E}{(1+\nu)} \frac{A_{ij}}{h_{ij}}$$

and rotational stiffness according to each local axis is as follows:

$$k_{\phi n} = \frac{EJ_p}{h_{ij}}, k_{\phi s} = \frac{EI_{22}}{h_{ij}}, k_{\phi n} = \frac{EI_{11}}{h_{ij}} \quad (2)$$

where E is concrete elastic modulus, ν is Poisson's ratio, h_{ij} is length of element ij , A_{ij} is Voronoi facet area of element ij , J_p is polar moment of inertia, and I_{11} and I_{22} are principal moments of inertia.

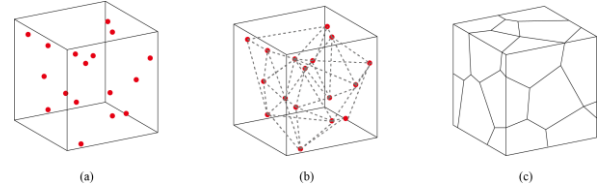


Figure 1: RBSN mesh generation: (a) Random point generation; (b) Delaunay tessellation; (c) Voronoi tessellation

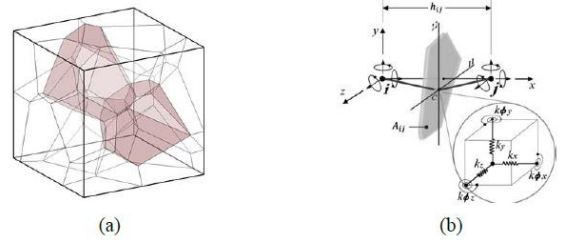


Figure 2: RBSN element: (a) Two-cell assembly; (b) RBSN element [9]

2.2 Visco-Plastic-Damage(VPD) model

Concrete is a rate dependent material that its properties such as strength and elastic modulus change according to the rate of loading. This has been demonstrated in many different researches as shown in Figure 3 [10]. Therefore, such physical mechanism has to be considered to conduct an analysis of dynamic loading on the rate dependent materials such as concrete. Realistic modeling of the rate dependency in concrete is difficult due to the intricacy of the physical mechanisms, some of which occur in the microscopic level. So microscopic material model has employed rheological devices (Figure 4) with viscosity term to reproduce the rate effects [11, 12].

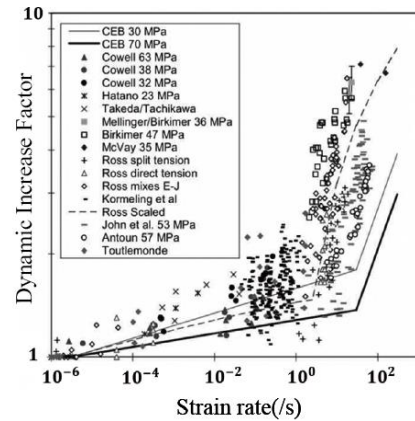


Figure 3: Various experimental data regarding dynamic increase factor for tensile strength [10]

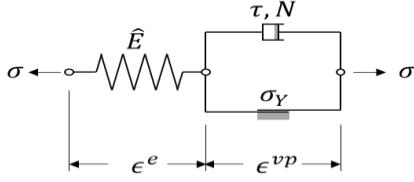


Figure 4: Schematic rheological model of viscoplasticity

2.3 Semi-discrete method

To indicate the stiffness of a fiber passing through a Voronoi cell, the semi-discrete method was used. The semi-discrete method accounts for fiber behavior by inserting a spring at the location of fiber intersection with the Voronoi facet. Applying this method is computationally efficient when generating great amount of fibers like in case of FRCCs because creating additional degrees of freedom is not required [6, 7].

2.4 Fiber pullout

The fiber crack bridging stress when the pullout force is being applied on the fiber can be expressed in two different states, before and after the debonding of the fiber/matrix interface. The calculation of the debonding and pullout was done using equations from Lin et al (1999) [13]. The calculation of the bridging stress, σ_{debond} , in the debonding stage is as follows.

$$\sigma_{debond} = 2 \sqrt{(\tau_0 u + G_d) \frac{2E_f(1 + \eta)}{d_f}} \quad (3)$$

where τ_0 is constant frictional stress, G_d is debonding fracture energy, η is ratio of fiber stiffness to effective matrix stiffness, E_f is fiber elastic modulus, and d_f is fiber diameter. The fiber stress, $\sigma_{pullout}$, at the fiber pullout stage after the complete fiber debonding was calculated as follows.

$$\sigma_{pullout} = \frac{\tau_0}{d_f} (L_e - u - \delta_c) \left[1 + \frac{\beta(u - \delta_c)}{d_f} \right] \quad (4)$$

$$\delta_c = \frac{\tau_0 L_e^2 (1 + \eta)}{E_f d_f} + \sqrt{\frac{8G_d L_e^2 (1 + \eta)}{E_f d_f}} \quad (5)$$

where L_e is the fiber embedment length, β is

slip-hardening coefficient, and δ_c is the displacement when the complete debonding of the fiber occurs. The fiber pullout behavior according to β , calculated using equations 4 and 5, is shown in Figure 5.

To test the rate dependency of fiber/matrix interface, Yang and Li (2006) conducted a single fiber pullout test with the pullout speed ranging from 10^{-3} to 10 mm/s [14]. In the test, three interface properties, which are chemical bond strength (G_d), frictional bond strength (τ_0), and slip hardening coefficient (β), were considered. The test results showed that the strain rate greatly affects the chemical bond strength; however, the friction bond strength and the slip hardening coefficient did not show any rate dependency within the speed range of 10^{-3} to 10 mm/s. Therefore, the chemical bond strength is the only factor among the interface properties that it changes based on the pullout speed. In addition, the change in the general properties, such as the elastic modulus and strength, of the fiber has to be considered as well.

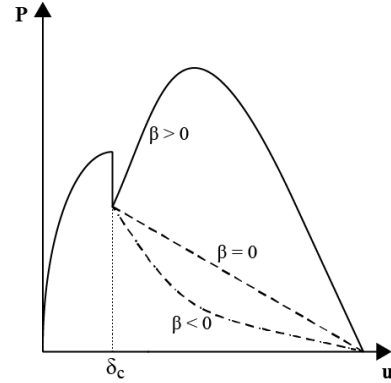


Figure 5: Fiber pullout behavior: $\beta=0$ interface friction is independent of slip distance; and $\beta<0$ softening; $\beta>0$ hardening

3 SINGLE FIBER PULLOUT TEST

According to Gokoz and Naaman (1981), the pullout behavior of a smooth steel fiber is independent to the pullout speed [15]. Therefore, in this research, an analysis, only considering the rate dependency of a matrix, was conducted with the range of pullout speed that was used in the actual experiments. Gokoz and Naaman (1981) used the test specimen

shown in Figure 6. The cylindrical specimen had 20 smooth fibers evenly spaced and embedded in parallel. In this research, to verify the results of the single fiber pullout, the analysis was conducted as shown in Figure 7, assuming that the pullout stress is proportional to the number of fibers. The loading rates of the pullout analysis were ranged from 4.2×10^{-3} cm/sec to 300cm/sec.

The material properties of a smooth steel fiber used in the pullout test, were arbitrarily assumed. And by conducting the analysis, accuracy of the developed analysis program in terms of rate dependency of a matrix and generation of a fiber was confirmed.

In addition, to consider the rate dependency of the fiber/matrix interface, a material, with chemical bond strength not equal to zero, was used in the analysis. Yang and Li (2014) conducted the analysis on the rate dependency of the interface properties based on the PVA fiber single pullout test, which is the test conducted with strain rate of 10^{-5} to $10^{-1} s^{-1}$ on the $10 \times 5 \times 0.5$ mm matrix (Figure 8). The mechanical properties of the PVA fiber are listed on Table 1.

Based on the experiment settings, an analysis was conducted. Furthermore, according to the results of the fiber pullout analysis about different loading rates, methods to depict the dynamic behavior of a fiber were researched.

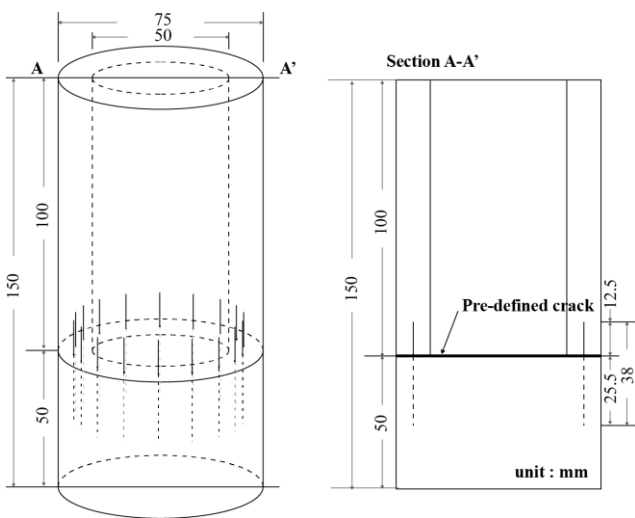


Figure 6: Pullout specimen [15]

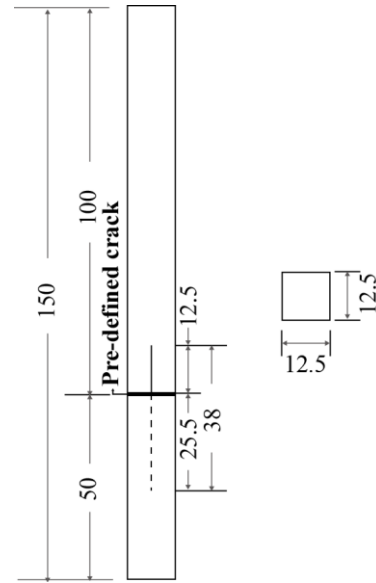


Figure 7: Single pullout test of smooth steel fiber

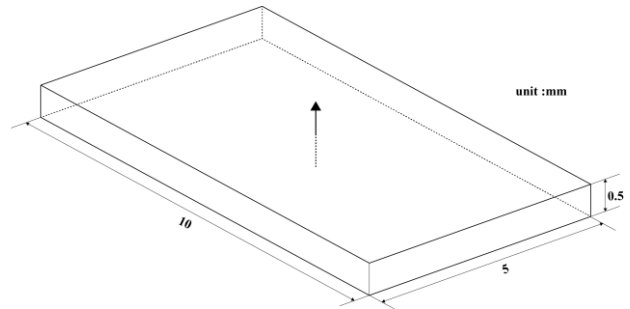


Figure 8: Geometry for single fiber pullout test

Table 1: Mechanical properties of PVA fibers

| Diameter (μm) | Tensile strength (MPa) | Tensile modulus (GPa) | τ_0 (MPa) | β |
|---------------|------------------------|-----------------------|----------------|---------|
| 40 | 1600 | 42 | 5.9 | 0.4 |

4 CONCLUSION

The dynamic analysis on reinforced concrete using semi-discrete method has been completed on Figure 9. Fiber analysis module was developed using the equations (3)-(5), however, the rate-dependency of fibers was not considered in these equations and fiber pull-out mechanism according to the dynamic loading is still difficult to be expressed in the module. In the case of the material which is dependent to pull-out speed, parametric studies by changing the interfacial property expressed in terms of chemical bond energy on the equations (3)-(5) are in progress.

Also, the implementation of visco-plastic term to the fiber interfacial property are in consideration.

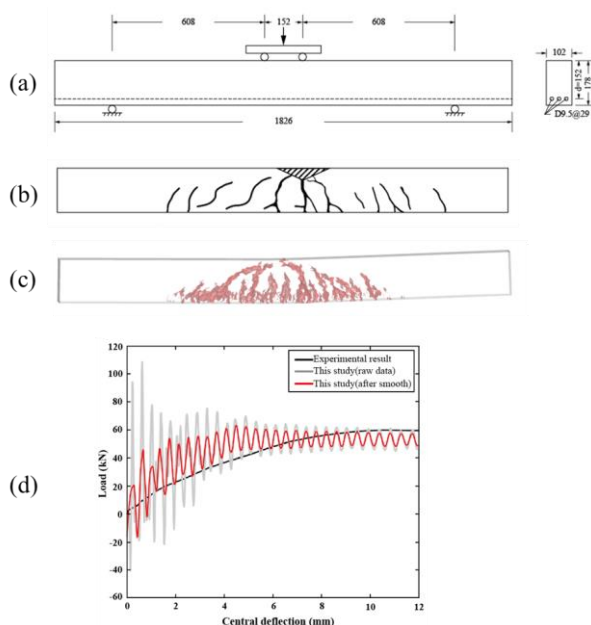


Figure 9: Four-point bending test of reinforced concrete beam against loading velocity of 380mm/s: (a) Test specimen configuration; (b) Crack pattern of experimental specimen; (c) Crack pattern of simulation result; (d) Central deflection-load curve

5 ACKNOWLEDEMENT

This research was supported by the Education-research Integration through Simulation On the Net (EDISON) Program through the National Research Foundation of Korea (NRF) funded by the Ministry of Science, ICT & Future Planning (NRF-2014M3C1A6038855) and supported by the Korea Institute of Energy Technology Evaluation and Planning (KETEP) granted financial resource from the Ministry of Trade, Industry & Energy, Republic of Korea (No.20171510101910).

REFERENCES

- [1] Bischoff, P. H., and Perry, S. H. 1991. Compressive behavior of concrete at high strain rates. *Material and structures* **24(6)**:424-450.
- [2] Yu, R.C. and Ruiz, G., 2006. Explicit finite element modeling of static crack propagation in reinforced concrete. *Int. J.*

Fract. **141**:357-72.

- [3] Malvar, L. J., and Ross, C. A. 1998. Review of strain rate effects for concrete in tension. *Materials Journal* **95(6)**:735-739.
- [4] Kim, K., and Lim, Y. M. 2011. Simulation of rate dependent fracture in concrete using an irregular lattice model. *Cement and Concrete Composites* **33(9)**:949-955.
- [5] Hwang, Y. K., and Lim, Y. M. 2017. Validation of three dimensional irregular lattice model for concrete failure model simulations under impact loads. *Engineering Fracture Mechanics* **169**:109-127.
- [6] Bolander, J. E., Hong, G. S., and Yoshitake, K. 2000. Structural concrete analysis using rigid-body-spring networks. *Computer-Aided Civil and Infrastructure Engineering* **15(2)**:120-133.
- [7] Mien, Y., Mohle, J., and Bolander, J. E. 2005. Automated modeling of three-dimensional structural component using irregular lattices. *Computer-Aided Civil and Infrastructure Engineering* **20(6)**:393-407.
- [8] Clifton JR. 1984. Penetration resistance of concrete – a review. *Washington (DC): National Bureau of Standards* 480-45.
- [9] Yip, M., Mohle, J., and Bolander, J. E. 2005. Automated modeling of three-dimensional structural components using irregular lattices. *Computer-Aided Civil and Infrastructure Engineering* **20(6)**:393-407.
- [10] Malvar, L. J., and Ross, C. A. 1998. Review of strain rate effects for concrete in tension. *Materials Journal* **95(6)**:735-739.
- [11] Kim, K., Bolander, J. E., and Lim, Y. M. 2011. Rigid-body-spring network with visco-plastic damage model for simulating rate dependent fracture of RC structures. *Applied Mechanics and Materials* (Trans Tech Publications) **82**:259-265.
- [12] Hwang, Y. K., Kim, K., Bolander, J. E., and Lim, Y. M. 2015. Evaluation of rheological models within lattice-based simulations of concrete under dynamic loading. *Proceedings of 5th International Workshop on Performance, Protection & Strengthening of Structures under Extreme*

Loading 36-43.

- [13] Lin, Z., Kanda, T., and Li, V. C. 1999. On interface property characterization and performance of fiber reinforced cementitious composites.
- [14] Yang, E., and Li, V. C. 2006. Rate dependence in engineered cementitious composites. *International RILEM workshop on high performance fiber reinforced cementitious composites in structural applications (RILEM Publications SARL)* 83-92.
- [15] Gokoz, U. N., and Naaman, A. E. 1981. Effect of strain-rate on the pull-out behaviour of fibres in mortar. *International Journal of Cement Composites and Lightweight Concrete* **3(3)**: 187-202.
- [16] Yang, E. H., and Li, V. C. 2014. Strain-rate effects on the tensile behavior of strain-hardening cementitious composites. *Construction and Building Materials* **52**:96-104.